Hindawi Publishing Corporation
Journal of Nanomaterials
Volume 2016, Article ID 3797896, 8 pages
http://dx.doi.org/10.1155/2016/3797896

*Research Article*

# Impact of Precipitants on the Structure and Properties of Fe-Co-Ce Composite Catalysts

**Yongli Zhang,[1] Shujuan Dai,[2] Yanbo Zhou,[1] and Kai Lin[1]**

[1]*School of Chemical and Environmental Engineering, Hanshan Normal University, Chaozhou 521041, China*
[2]*School of Mining Engineering, University of Science and Technology Liaoning, Anshan 114051, China*

Correspondence should be addressed to Shujuan Dai; shujuandai@163.com

Received 11 January 2016; Accepted 13 March 2016

Academic Editor: Vincenzo Baglio



Fe-Co-Ce composite catalysts were prepared by coprecipitation method using $CO(NH_2)_2$, NaOH, $NH_4HCO_3$, and $NH_3{\cdot}H_2O$ as precipitant agents. The effects of the precipitant agents on the physicochemical properties of the Fe-Co-Ce based catalysts were investigated by SEM, TEM, BET, TG-DTA, and XRD. It was found that the precipitant agents remarkably influenced the morphology and particle size of the catalysts and affected the COD removal efficiency, decolorization rate, and pH of methyl orange for catalytic wet air oxidation (CWAO). The specific surface area of the Fe-Co-Ce composite catalysts successively decreased in the order of $NH_3{\cdot}H_2O$, $NH_4HCO_3$, NaOH, and $CO(NH_2)_2$, which correlated to an increasing particle size that increased for each catalyst. For the CWAO of a methyl orange aqueous solutions, the effects of precipitant agents $NH_3{\cdot}H_2O$ and NaOH were superior to those of $CO(NH_2)_2$ and $NH_4HCO_3$. The catalyst prepared using $NH_3{\cdot}H_2O$ as the precipitant agent was mostly composed of $Fe_2O_3$, CoO, and $CeO_2$. The COD removal efficiency of methyl orange aqueous solution for $NH_3{\cdot}H_2O$ reached 92.9% in the catalytic wet air oxidation. Such a catalytic property was maintained for six runs.

## 1. Introduction

A large amount of wastewater is produced worldwide every year from the ever-expanding printing and dyeing industries. The wastewater originating printing and dyeing industries contain potentially dangerous dyes, dye auxiliaries, acids, alkali metals, and organic compounds [1]. Due to the high concentrations of these above-mentioned compounds, complex composition, and poor degradability, it is difficult to treat printing and dyeing wastewater. As a result, current methods and equipment used for treatment have stringent requirements. On the other hand, it is difficult to treat wastewater by conventional methods [2]. Catalytic wet air oxidation (CWAO), which is an advanced oxidation technology, has shown great potential for the treatment of biorefractory wastewater. Therefore, researchers have shown profound interest in the research of catalysts [3]. It is well known that the noble metal catalysts have excellent catalytic performance. However, owing to their high cost and low natural occurrence, their industrial production and applications are hindered [4]. Therefore, many researchers in the field of CWAO have focused on searching for alternative nonnoble metal catalysts with lower price, higher activity, and better stability [5]. On the other hand, transition metals are widely used in industrial production and application due to their ubiquitous presence, relatively low cost, and outstanding catalytic performance [6]. Rare earth metals can be combined with transition metals to form multicomponent catalysts, which will generate synergistic effects due to their special physical and chemical properties. Therefore, rare earth metals have been increasingly investigated for use with transition metals for researchers investigating catalysts [7].

Currently, the methods for synthesizing catalysts include impregnation [8], coprecipitation method [9], and sol-gel method [10]. The coprecipitation method is widely applied in industrial production because of its advantages of simple operation, convenient large-scale manufacturing, and ease of morphology control. The selection of precipitant agents plays an important role for the preparation of composite catalysts [11]. For example, Zhang et al. [12] used $NH_3{\cdot}H_2O$, $Na_2CO_3$, $NaHCO_3$, NaOH, and $(NH_4)_2CO_3$ as precipitant agents,

respectively, to prepare $MgO/SnO_2/WO_3$ catalysts, and they were used for synthesizing epsilon caprolactone. Specifically, the catalyst prepared by the $NH_3{\cdot}H_2O$ precipitant agent exhibited excellent catalytic performance. Park et al. [13] prepared CuO catalysts using $NH_3{\cdot}H_2O$, $NaHCO_3$, $Na_2CO_3$, and NaOH as precipitant agents and found that $HCO_3^-$ and $CO_3^{2-}$ weaken the Cu-O chemical bond in the presence of $Na^+$ on the CuO surface and accelerate the mobility of oxygen and the formation of lattice oxygen. Wang et al. [14] prepared Ni-$CeO_2$ catalyst by coprecipitation method using $Na_2CO_3$, NaOH, and a $Na_2CO_3$-NaOH mixture (molar ratio of 1 : 1) as a precipitant agent. The mixed precipitant had plenty of oxygen vacancies accompanied with highly dispersed Ni particles and exhibited high catalytic activity. Taken as a whole, it is important to prepare a catalyst with high catalytic performance that is also nonpolluting at the same time.

Building on the previous research, the Fe-Co-Ce composite catalysts were prepared by the coprecipitation method with iron nitrate, cobalt nitrate, and cerium nitrate as metal sources in the present study [15]. Transition metals Fe and Co were used as the main components of the catalyst [16, 17], and rare earth metal Ce was used as catalyst promoter [18]. The present study aims at investigating the effects of $CO(NH_2)_2$, NaOH, $NH_4HCO_3$, and $NH_3{\cdot}H_2O$ on the particle size and morphology and structure characteristic of the Fe-Co-Ce composite catalysts. The influence of different precipitants on the chemical oxygen demand (COD) removal efficiency, decolorization rate, and pH of methyl orange in CWAO over the Fe-Co-Ce composite catalysts was also investigated.

## 2. Experimental

*2.1. Catalyst Preparation.* The Fe-Co-Ce composite catalysts were prepared by coprecipitation method, with a metal atom ratio of 1 : 1 : 1 in Fe : Co : Ce. A specific amount of $Fe(NO_3)_3{\cdot}9H_2O$, $Co(NO_3)_2{\cdot}6H_2O$, and $Ce(NO_3)_3{\cdot}6H_2O$ (AR grade, Aladdin Reagent Co., Ltd.) was weighed, mixed in 100 mL distilled water, and stirred to create a homogenous solution with a concentration of 0.2 M. The precipitant agents $CO(NH_2)_2$, NaOH, $NH_4HCO_3$, and $NH_3{\cdot}H_2O$ were added to the mixed solution with a concentration of 1.5 M at a speed of 6 drops/min. The sample was magnetically stirred at medium intensity until white precipitants were generated and the pH of the mixed solution reached the equilibrium critical point of 6, 11, 8, and 10. Then, white precipitants were aged at room temperature for 2 h, and the resulting products were poured into a Buchner Funnel, washed twice with distilled water, and collected by vacuum filtration. Subsequently, the samples were dried at 105°C for 10 h with ventilation and calcined at 550°C for 3 h at a heating rate of 10°C/min. This precipitation-calcination was repeated twice to ensure complete loading. Finally, the Fe-Co-Ce composite catalyst powders were ground in a crucible, and they were marked as CAT-1, CAT-2, CAT-3, and CAT-4, corresponding to the precipitant agents $CO(NH_2)_2$, NaOH, $NH_4HCO_3$, and $NH_3{\cdot}H_2O$, respectively.

*2.2. Catalyst Characterization.* The surface morphology and energy dispersive X-ray spectroscopy (EDS) of the samples were observed by means of a scanning electron microscope (ZEISS Auriga FIB, Germany). The surface particle size and structure of the samples were obtained on a transmission electron microscope (TEM, JEOL JEM-3010). The surface and pore structure were determined using a physical adsorption instrument (ASAP2400, Micrometrics, USA) at −196°C. The samples were treated for 4 h under vacuum and 180°C before analysis. Thermogravimetry differential thermal analysis (TG-DTA) experiments were performed by a simultaneous thermal analyzer (EXSTAR-7000, Japan). The phase compositions of the samples were measured by a Rigaku D/Max-2400 X-ray diffractometer (XRD) with Cu $K\alpha$ radiation at 40 kV, 100 Ma, and 6°/min.

*2.3. Catalyst Test.* CWAO experiments treating methyl orange (25 mg/L) were performed in 0.5 L batch autoclave (GS-0.5, Weihai, China) with 2 g/L catalyst. Pure oxygen was pumped into the reactor with continuous heating until the reaction temperature and oxygen partial pressure were 180°C and 2.5 MPa, respectively. The device had a stirring rate of 500 rpm, and 20 mL aqueous solutions were taken for analyses at 10, 20, 40, 60, and 90 min. The catalytic performance was evaluated by the COD removal efficiency and decolorization rate of aqueous solutions. The COD of water samples was measured by the national standard method of potassium dichromate and absorbance of aqueous solutions was measured using a spectrophotometer. And the decolorization rate of aqueous solutions was calculated by the following formula:

$$\text{Decolorization } (\%) = \frac{A_0 - A_t}{A_0} \times 100\%, \tag{1}$$

where $A_0$ represents the initial absorbance and $A_t$ stands for the absorbance at time $t$.

## 3. Results and Discussion

*3.1. SEM and EDS Analyses.* The SEM images and EDS analyses of the Fe-Co-Ce composite catalysts, prepared using $CO(NH_2)_2$, NaOH, $NH_4HCO_3$, and $NH_3{\cdot}H_2O$ as a precipitant agent, are shown in Figures 1(a)–1(d), respectively. Figure 1 shows the four types of catalysts under the above four precipitant agents, which were mainly composed of spherical-like and plate-like grains. The CAT-1 particles displayed obvious agglomeration and larger particle size, whereas the particles of CAT-2 mainly consisted of a flaky structure presumably because the formation of the crystalline grain was rapid under the strong alkalinity of NaOH [19]. The particles of CAT-3 were quasi-spherical with a distinct profile and were poorly dispersed. The particles of CAT-4 were quasi-spherical too, but the particle size was smaller than that of CAT-3. The smaller particle size of CAT-4 could be due to the fact that the alkalinity of $OH^-$ was higher than that of $HCO_3^-$ in $NH_3{\cdot}H_2O$ which may have resulted in a rapid precipitation process. Figure 1(e) shows that, under the condition of ammonia precipitation, the atomic ratio of

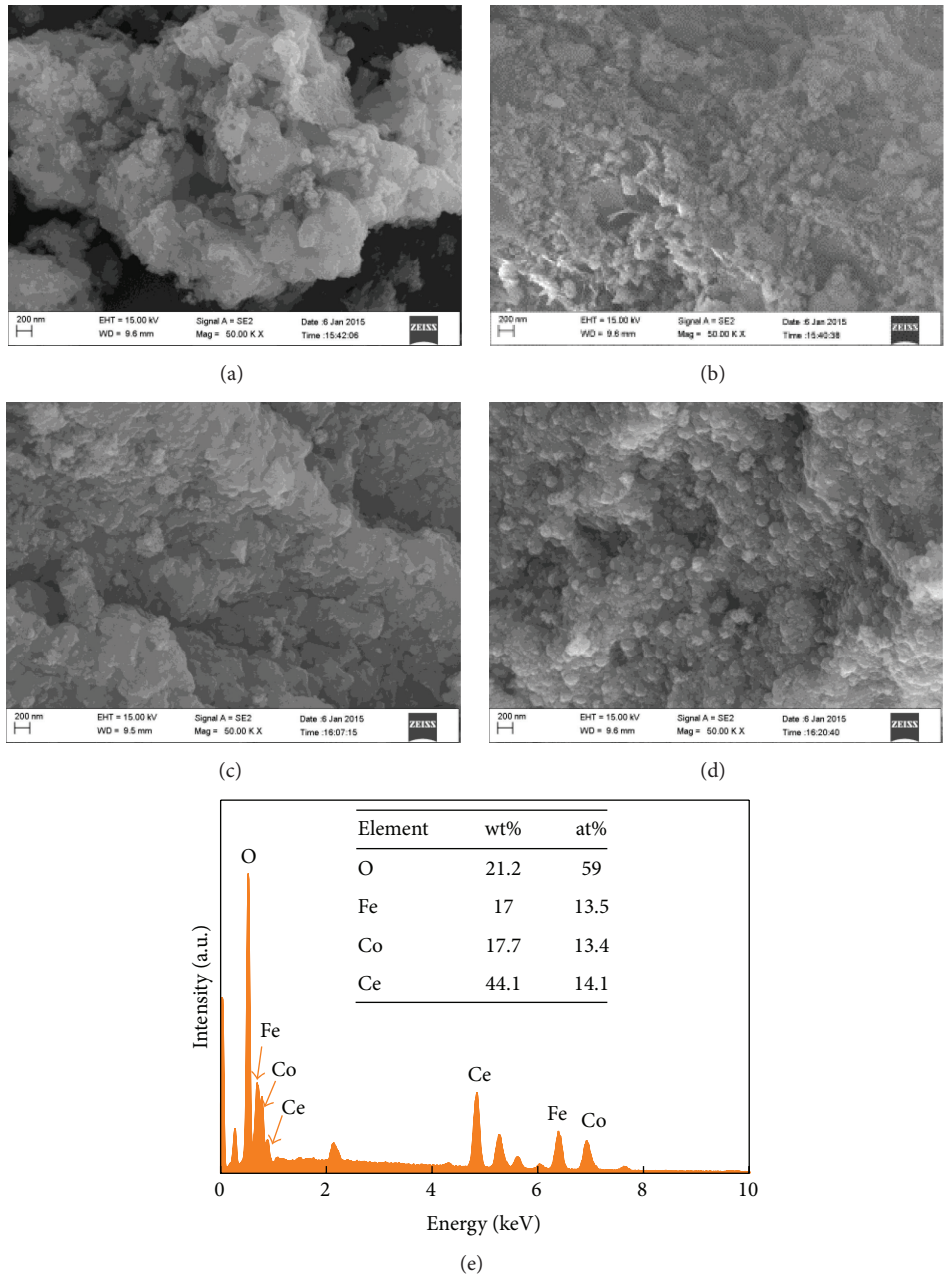


Figure 1: SEM (a–d) images and EDS (e) analysis of the Fe-Co-Ce composite catalysts prepared using various precipitants: (a) $CO(NH_2)_2$, (b) NaOH, (c) $NH_4HCO_3$, and (d, e) $NH_3{\cdot}H_2O$.

Fe : Co : Ce was approximately 1 : 1 : 1, which was consistent with the mass fraction of Fe, Co, and Ce that was 17.0%, 17.7%, and 44.1%, respectively.

*3.2. TEM and Particle Size Analyses.* Figure 2 shows the TEM images and the metal nanoparticle size distribution histograms of the Fe-Co-Ce composite catalysts prepared using the four precipitant agents. As shown in Figures 2(a), 2(c), 2(e), and 2(g), the particle size of CAT-1 was larger than that of other samples due to agglomeration with an ambiguous crystal profile having an average particle size of 11.0 nm. The crystalline grain generation rate of CAT-2 was rapid with partial agglomeration due to the strong alkalinity of NaOH, and an average particle size of 10.1 nm was observed. Both particles of CAT-3 and CAT-4 exhibited clear boundaries, and CAT-3 had a relatively complete shape. On the other hand, the particles of CAT-4 were evenly distributed on the catalyst surface, and the average particle sizes of CAT-3 and CAT-4 were 7.3 nm and 6.8 nm, respectively.

*3.3. Analysis of Pore Structure.* For further investigating the influence of precipitant agents on the specific surface area and

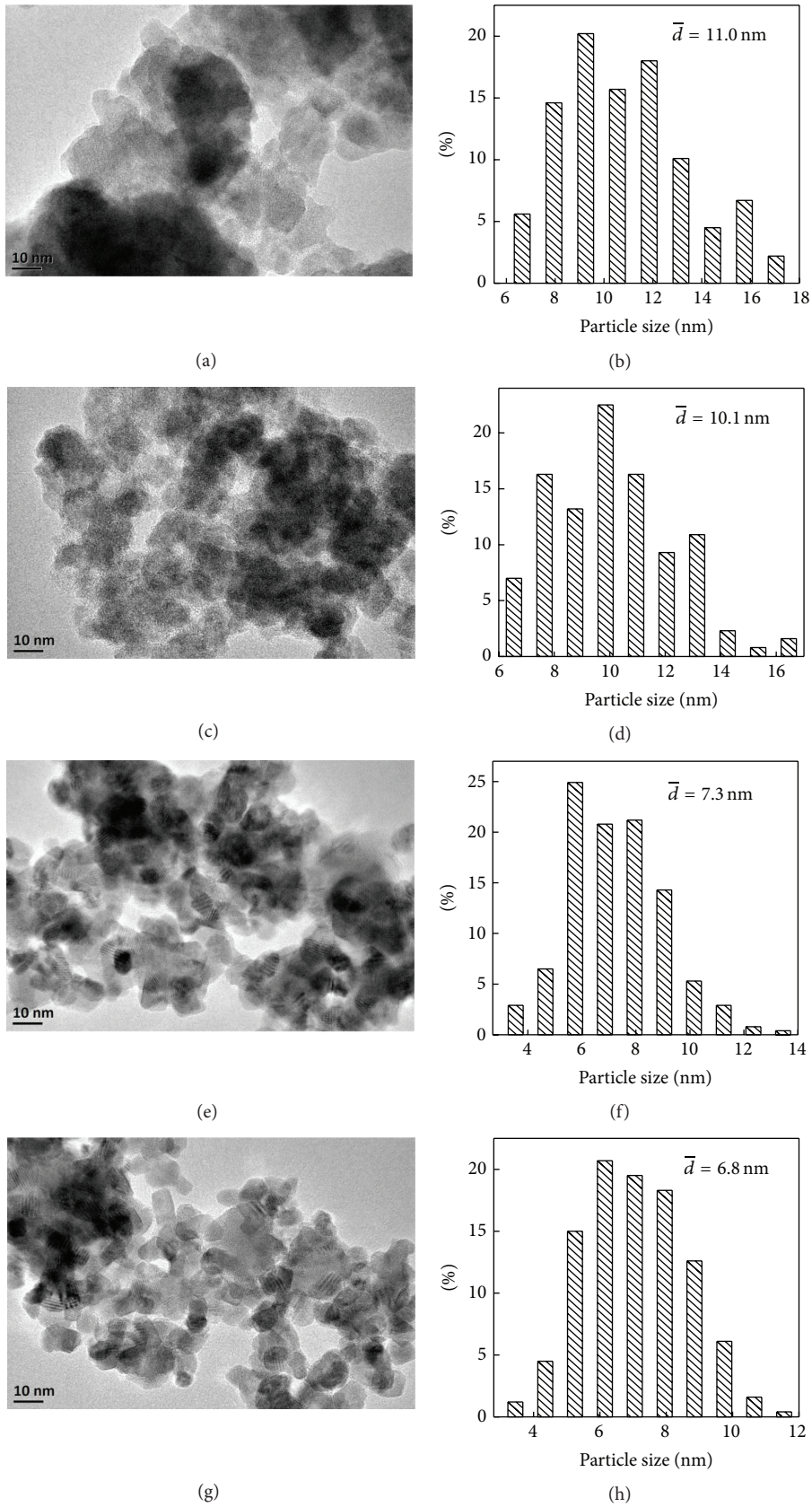


Figure 2: TEM images and the metal nanoparticle size distribution histograms of the Fe-Co-Ce composite catalysts prepared using various precipitants: (a, b) $CO(NH_2)_2$; (c, d) NaOH; (e, f) $NH_4HCO_3$; and (g, h) $NH_3 \cdot H_2O$.

Table 1: Pore structures of the Fe-Co-Ce composite catalysts prepared using various precipitants.

| Sample | CAT-1 | CAT-2 | CAT-3 | CAT-4 |
|---|---|---|---|---|
| Special surface area/$m^2 \cdot g^{-1}$ | 45.84 ± 1.2 | 66.72 ± 2.2 | 71.49 ± 1.8 | 83.87 ± 3.1 |
| Pore volume/$cm^3 \cdot g^{-1}$ | 0.15 ± 0.006 | 0.13 ± 0.004 | 0.12 ± 0.004 | 0.14 ± 0.005 |
| Average pore diameter/nm | 8.23 ± 0.2 | 6.95 ± 0.1 | 6.76 ± 0.2 | 6.63 ± 0.1 |

pore size distribution of the Fe-Co-Ce composite catalysts, the catalysts were characterized by nitrogen adsorption-desorption technique (Table 1). The specific surface area of CAT-1, CAT-2, CAT-3, and CAT-4 exhibited an ascending trend, with values of 45.84, 66.72, 71.49, and 83.87 $m^2/g$, respectively. Conversely, an opposite trend was observed for the variation in pore size. CAT-4 with the $NH_3 \cdot H_2O$ precipitant agent had the largest specific surface area but the smallest pore size probably attributed to the fact that using alkalescent $NH_3 \cdot H_2O$ as the precipitant agent could have resulted in an appropriate nucleation rate, possibly generating a smaller grain size and more homogeneous distribution.

*3.4. Degradation Performance of Methyl Orange.* Figures 3(a)–3(c) show the COD removal efficiencies, decolorization rates, and pH for CWAO of methyl orange aqueous solutions over the Fe-Co-Ce composite catalysts prepared using the four precipitant agents, respectively. The COD removal efficiencies for methyl orange aqueous solutions after 90 min were 62.7%, 94.3%, 77.2%, and 92.9%, using CAT-1, CAT-2, CAT-3, and CAT-4, respectively. The COD removal efficiencies of the Fe-Co-Ce composite catalysts prepared using $NH_3 \cdot H_2O$ or NaOH as the precipitant agent were higher than those prepared using $CO(NH_2)_2$ and $NH_4HCO_3$. Notably, using NaOH as the precipitant agent resulted in the introduction of $Na^+$ into the aqueous solutions, which adversely affected effluent quality [20]. Figure 3(b) shows the decolorization rates of the methyl orange aqueous solutions in the CWAO over the catalysts prepared by the four precipitant agents. The trend of the decolorization rates was consistent with that of the COD removal efficiencies, and the decolorization rates of CAT-1, CAT-2, CAT-3, and CAT-4 were 81.4%, 99.8%, 86.7%, and 99.6%, respectively.

Figure 3(c) illustrates that the pH of methyl orange aqueous solutions continually decreased in 90 min when treated with CAT-1 and CAT-3 catalysts. The pH of the methyl orange aqueous solutions increased after an initial decline when treated with CAT-2 and CAT-4. Methyl orange present in water can degrade to an organic acid, resulting in a low pH until the organic acid further decomposed into $CO_2$, $H_2O$, $N_2$, and other small inorganic molecules, which then gradually results in increasing pH. After a treatment time of 90 min, the pH of the samples differed in the order of CAT-2 > CAT-3 > CAT-4 > CAT-1, with end point pH values of 5.7, 5.6, 4.9, and 4.6, respectively. The increase of the catalyst specific surface area was beneficial for increasing the effective contact area between the sample and methyl orange aqueous solution which in turn improved the ability of the catalyst to degrade the pollutants. From the above results, we can conclude that the particle sizes and pore structures of the catalyst affect the degradation of methyl orange. Therefore, $NH_3 \cdot H_2O$ was determined to be the most appropriate among the above four precipitants used in this study.

### *3.5. Physicochemical Properties of Catalyst Using the Ammonia Precipitant Agent*

*3.5.1. TG-DTA Result.* In order to further investigate the catalyst structure under optimal precipitation condition, the TG-DTA of the Fe-Co-Ce composite catalyst prepared using $NH_3 \cdot H_2O$ precipitant agent was analyzed and the results are shown in Figure 4. As shown in the DTA curve, two obvious endothermic peaks were observed at 186.8°C and 230.4°C, respectively, in the range of 0°C to 900°C. The TG curve was divided into three stages, with a large weight loss in the interval ranging from 0°C to 186.8°C, which indicated the loss of the adsorbed water. The second significant weight loss that occurred in the interval 186.8°C to 230.4°C was attributed to nitrate decomposition. A small amount of mass loss occurred in the range of 230.4°C to 900°C, attributed to the further decomposition of oxides. According to the above analyses, the catalyst was calcined at 550°C and with a stable chemical composition mainly containing metal oxides.

*3.5.2. XRD Result.* The XRD pattern of the Fe-Co-Ce composite catalyst prepared using the $NH_3 \cdot H_2O$ precipitant is displayed in Figure 5. Diffraction peaks were observed at 28.6°, 33.1°, 47.5°, 56.3°, 59.1°, 69.4°, 76.7°, 79.1°, and 88.4° corresponding to the (111), (200), (220), (311), (222), (400), (311), (420), and (422) crystal planes of $CeO_2$ (JCPDS 34-0394), respectively. Sharp and intense diffraction peaks were observed, indicating high crystallinity and $CeO_2$ content. The weak peaks that appeared at $2\theta$ of 33.1° (104), 35.6° (110), and 62.4° (214) were indexed to the crystal planes of $Fe_2O_3$ (JCPDS 99-0060). This result suggests that the amount of $Fe_2O_3$ was low or the particles of $Fe_2O_3$ were uniformly distributed on the catalyst surface. Diffraction peaks characteristic of CoO (JCPDS 02-1217) were observed at $2\theta$ = 43.3°, 62.4° and 79.1°, indicating that Co exists on the catalyst surface in the form of CoO. Therefore, the catalysts are mainly composed of $Fe_2O_3$, CoO, and $CeO_2$, consistent with the results obtained from EDS and TG-DTA analyses.

*3.5.3. Stability and Recyclability.* The stability and recyclability of the Fe-Co-Ce composite catalyst prepared using the $NH_3 \cdot H_2O$ precipitant agent were investigated by repeatedly using it to degrade methyl orange tainted water. The results are shown in Figure 6, which indicates that the COD removal efficiency of methyl orange aqueous solutions reduced from 92.9% to 90.1% after six runs.

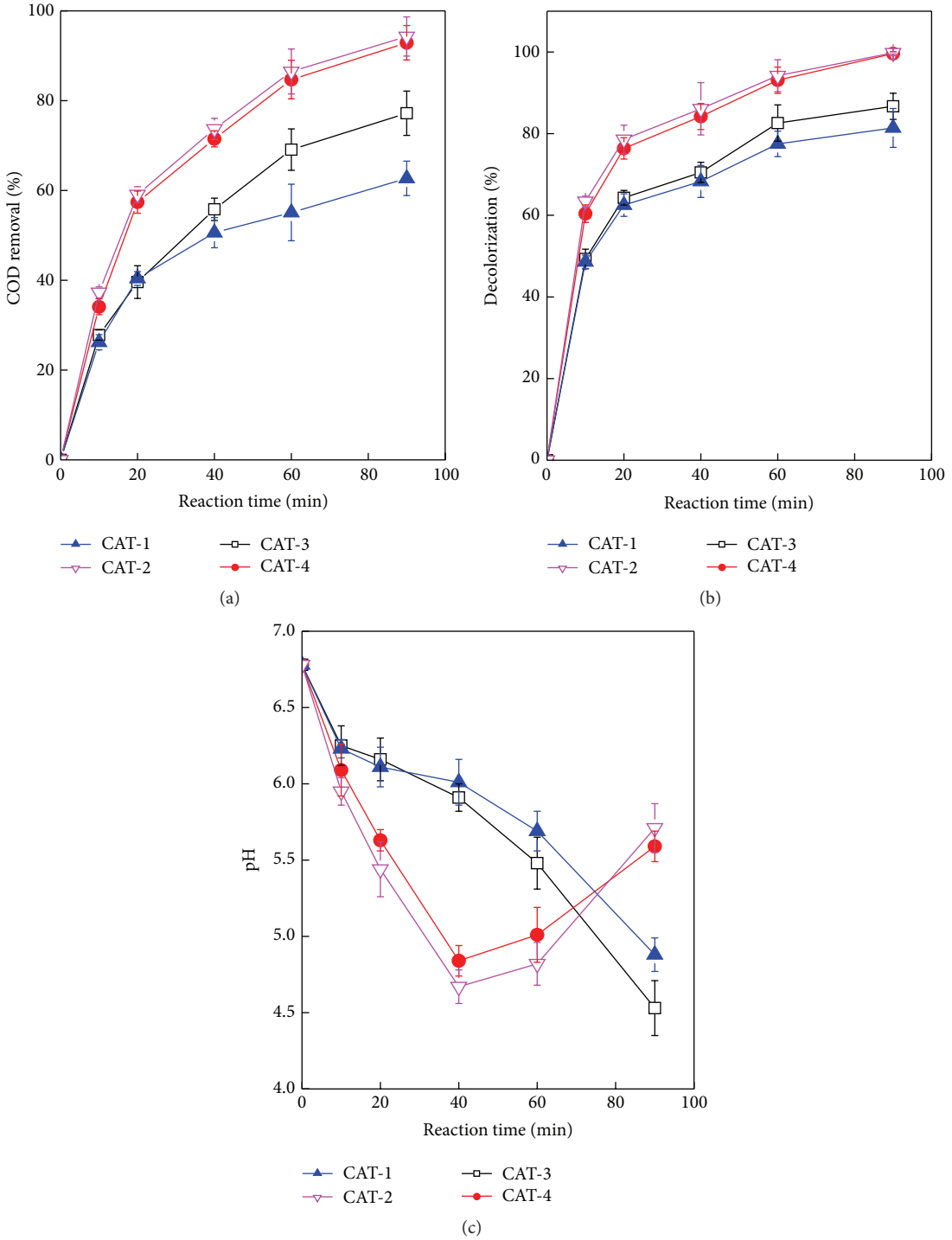


Figure 3: Activity curves of the Fe-Co-Ce composite catalysts prepared using various precipitants: (a) COD removal efficiency; (b) decolorization rate; and (c) pH.

Correspondingly, the decolorization rate decreased from 99.6% to 96.7% after six runs of 90 min each for the catalyst. This preliminary stability study supports the stability, limited activity loss, and repeatability of using the $NH_3{\cdot}H_2O$ precipitant agent to prepare Fe-Co-Ce composite catalyst in methyl orange degradation.

## 4. Conclusions

(1) Among the four Fe-Co-Ce composite catalysts prepared using $CO(NH_2)_2$, NaOH, $NH_4HCO_3$, and $NH_3{\cdot}H_2O$ as the precipitant agent in this study, the catalyst prepared using $CO(NH_2)_2$ exhibited a spherical-like structure with a particle aggregation and larger size. Notably, its nucleation rate was

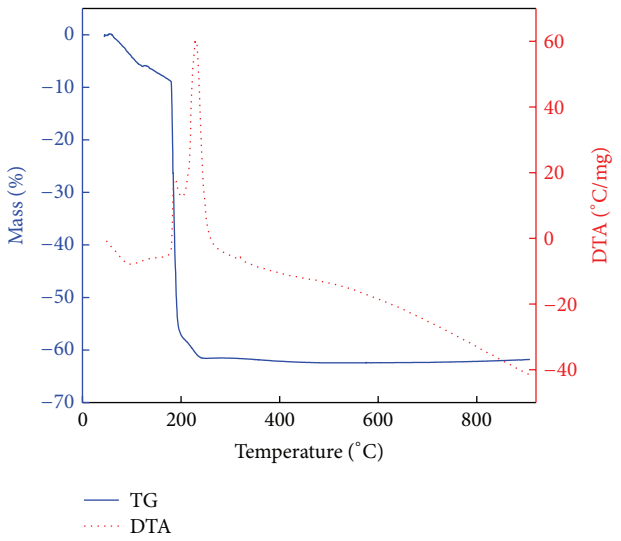


Figure 4: TG-DTA curves of the Fe-Co-Ce composite catalyst prepared using $NH_3{\cdot}H_2O$ precipitant.

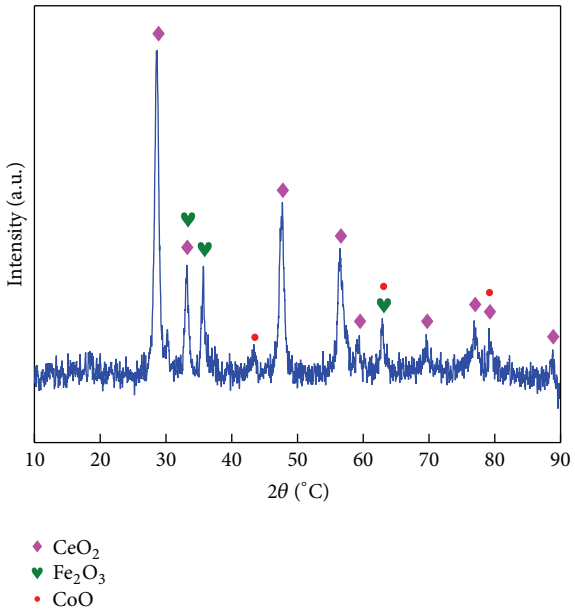


Figure 5: XRD spectrum of the Fe-Co-Ce composite catalyst prepared using $NH_3{\cdot}H_2O$ precipitant.

higher than that of the other three catalysts due to its strong alkalinity. When NaOH was used as the precipitant, the particles presented flaky structure and partial aggregation. Using the $NH_4HCO_3$ and $NH_3{\cdot}H_2O$ precipitant agents, the catalysts exhibited spherical-like particles with a distinct grain boundary. Using the $NH_4HCO_3$ precipitant, catalyst particles exhibited heterogeneous distribution, while, using the $NH_3{\cdot}H_2O$ precipitant agent, the catalyst particles exhibited a smaller average grain diameter of 6.8 nm and a larger specific surface area of 83.87 $m^2/g$.

(2) For the catalytic wet air oxidation of methyl orange aqueous solutions over the Fe-Co-Ce composite catalysts, the

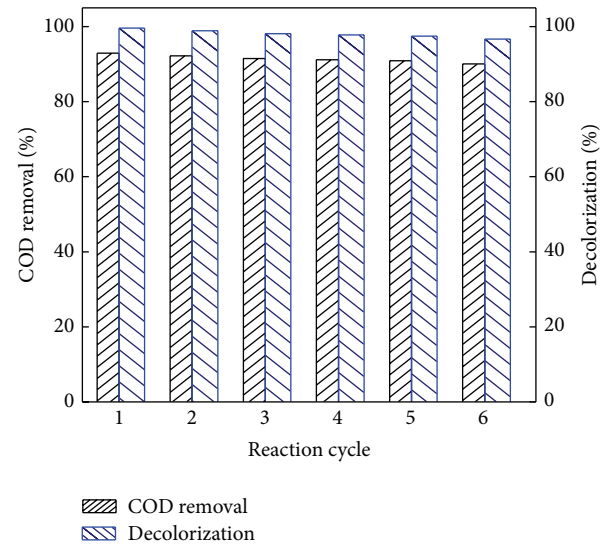


Figure 6: Recyclability histogram of the Fe-Co-Ce composite catalyst prepared using the $NH_3{\cdot}H_2O$ precipitant.

effects of the $NH_3{\cdot}H_2O$ and NaOH precipitant agents were superior to those of $CO(NH_2)_2$ and $NH_4HCO_3$ precipitant agents. The initial COD removal efficiency of the catalyst prepared using the $NH_3{\cdot}H_2O$ precipitant was 92.9% and the decolorization rate of methyl orange was 99.6%. After six runs using the same catalyst the COD removal efficiency of methyl orange was 90.1% and the decolorization was 96.7%. These data indicate that the Fe-Co-Ce composite catalyst prepared using the $NH_3{\cdot}H_2O$ precipitant exhibited excellent both initial and repeated ability to degrade methyl orange. (3) The active components of the Fe-Co-Ce composite catalyst prepared using $NH_3{\cdot}H_2O$ as the precipitant agent were mainly comprised of $Fe_2O_3$, CoO, and $CeO_2$.

## Competing Interests

The authors declare that they have no competing interests.

## Acknowledgments

This study was supported by the Started Project for Professor of Hanshan Normal University (QD20140615) and the China Postdoctoral Science Foundation (2014M552202).

## References

[1] H. Wu and S. Wang, "Impacts of operating parameters on oxidation-reduction potential and pretreatment efficacy in the pretreatment of printing and dyeing wastewater by Fenton process," *Journal of Hazardous Materials*, vol. 243, pp. 86–94, 2012.

[2] S. Roy and A. K. Saroha, "Ceria promoted $\gamma$-$Al_2O_3$ supported platinum catalyst for catalytic wet air oxidation of oxalic acid: kinetics and catalyst deactivation," *RSC Advances*, vol. 4, no. 100, pp. 56838–56847, 2014.

[3] Y. Xu, X. Li, X. Cheng, D. Sun, and X. Wang, "Degradation of cationic red GTL by catalytic wet air oxidation over Mo-Zn-Al-O catalyst under room temperature and atmospheric pressure," *Environmental Science and Technology*, vol. 46, no. 5, pp. 2856–2863, 2012.

[4] X. Ma, Y. Liu, X. Li, J. Xu, G. Gu, and C. Xia, "Water: the most effective solvent for liquid-phase hydrodechlorination of chlorophenols over Raney Ni catalyst," *Applied Catalysis B: Environmental*, vol. 165, pp. 351–359, 2015.

[5] J. Mazumder and H. I. de Lasa, "Fluidizable $La_2O_3$ promoted Ni/$\gamma$-$Al_2O_3$ catalyst for steam gasification of biomass: effect of catalyst preparation conditions," *Applied Catalysis B: Environmental*, vol. 168-169, pp. 250–265, 2015.

[6] S. He, L. Zhang, S. He et al., "Ni/$SiO_2$ catalyst prepared with nickel nitrate precursor for combination of $CO_2$ reforming and partial oxidation of methane: characterization and deactivation mechanism investigation," *Journal of Nanomaterials*, vol. 2015, Article ID 659402, 8 pages, 2015.

[7] I. Popescu, Y. Wu, P. Granger, and I.-C. Marcu, "An in situ electrical conductivity study of LaCoFe perovskite-based catalysts in correlation with the total oxidation of methane," *Applied Catalysis A: General*, vol. 485, pp. 20–27, 2014.

[8] F. Frusteri, M. Cordaro, C. Cannilla, and G. Bonura, "Multifunctionality of Cu–ZnO–$ZrO_2$/H-ZSM5 catalysts for the one-step $CO_2$-to-DME hydrogenation reaction," *Applied Catalysis B: Environmental*, vol. 162, pp. 57–65, 2015.

[9] F. Mauriello, H. Ariga, M. G. Musolino, R. Pietropaolo, S. Takakusagi, and K. Asakura, "Exploring the catalytic properties of supported palladium catalysts in the transfer hydrogenolysis of glycerol," *Applied Catalysis B: Environmental*, vol. 166-167, pp. 121–131, 2015.

[10] T. Melchiori, L. Di Felice, N. Mota et al., "Methane partial oxidation over a $LaCr_{0.85}Ru_{0.15}O_3$ catalyst: characterization, activity tests and kinetic modeling," *Applied Catalysis A: General*, vol. 486, pp. 239–249, 2014.

[11] G. Ovejero, A. Rodríguez, A. Vallet, and J. García, "Catalytic wet air oxidation of a non-azo dye with Ni/MgAlO catalyst," *Chemical Engineering Journal*, vol. 215-216, pp. 168–173, 2013.

[12] G. Zhang, X. Ren, H. Zhang, Y. Peng, and S. Gui, "MgO/$SnO_2$/$WO_3$ as catalysts for synthesis of $\varepsilon$-caprolactone over oxidation of cyclohexanone with peracetic acid," *Catalysis Communications*, vol. 58, pp. 59–63, 2015.

[13] J.-H. Park, J. H. Cho, K. H. Cho, T. W. Lee, H. S. Han, and C.-H. Shin, "CO oxidation over CuO catalysts prepared with different precipitants," *Korean Journal of Chemical Engineering*, vol. 29, no. 9, pp. 1151–1157, 2012.

[14] L. Wang, H. Liu, Y. Liu, Y. Chen, and S. Yang, "Effect of precipitants on Ni-$CeO_2$ catalysts prepared by a co-precipitation method for the reverse water-gas shift reaction," *Journal of Rare Earths*, vol. 31, no. 10, pp. 969–974, 2013.

[15] Y.-L. Zhang, C.-H. Wei, C. Shi, Z.-C. Huang, and X.-Y. Su, "Preparation, characterization and mechanism of Cu-Fe-Ru-La/$\gamma$-$Al_2O_3$ catalysts for wastewater wet oxidation," *Journal of Synthetic Crystals*, vol. 42, no. 7, pp. 1457–1469, 2013.

[16] S.-Y. Wang, N. Li, L.-F. Luo et al., "Probing different effects of surface $MO_y$ and $M^{n+}$ species (M = Cu, Ni, Co, Fe) for $xMO_y/Ce_{0.9}MM_{0.1-x}O_{2-\delta}$ catalysts in CO oxidation," *Applied Catalysis B: Environmental*, vol. 144, pp. 325–332, 2014.

[17] J. Li, G. Lu, G. Wu et al., "The role of iron oxide in the highly effective Fe-modified $Co_3O_4$ catalyst for low-temperature CO oxidation," *RSC Advances*, vol. 3, no. 30, pp. 12409–12416, 2013.

[18] J. M. Jacob, P. G. Corradini, E. Antolini, N. A. Santos, and J. Perez, "Electro-oxidation of ethanol on ternary Pt–Sn–Ce/C catalysts," *Applied Catalysis B: Environmental*, vol. 165, pp. 176–184, 2015.

[19] W. H. Tao, G. L. Ma, L. Zhou, and C. Rong, "Hydrothermal synthesis of $ZrO_2$-8 mol % $Y_2O_3$ nanocrystallites in basic media and electrical properties of their sinters," *Acta Chimica Sinica*, vol. 61, pp. 1955–1959, 2003.

[20] L. V. C. Lima, M. Rodriguez, V. A. A. Freitas et al., "Synergism between n-type $WO_3$ and p-type $\delta$-FeOOH semiconductors: high interfacial contacts and enhanced photocatalysis," *Applied Catalysis B: Environmental*, vol. 165, pp. 579–588, 2015.